UDC 004.891:528.4
DOI: http://doi.org/10.17721/1728-2713.110.13

Vasyl HUDAK[1], PhD Student
ORCID ID: 0009-0002-7333-0409
e-mail: gudak_vasyl@knu.ua

Serhii MARHES[2], PhD Student
ORCID ID: 0009-0004-2942-9406
e-mail: sergemarhes@gmail.com

Vitalii ZATSERKOVNYI[1], DSc (Techn.), Prof.
ORCID ID: 0009-0003-5187-6125
e-mail: vitalii.zatserkovnyi@knu.ua

Mauro DE DONATIS[3], PhD (Geol.), Assoc. Prof.
ORCID ID: 0000-0002-9721-1095
e-mail: mauro.dedonatis@uniurb.it

[1]Taras Shevchenko National University of Kyiv, Kyiv, Ukraine
[2]State Institution "Scientific Centre for Aerospace Research of the Earth of the Institute of Geological Sciences of the National Academy of Sciences of Ukraine", Kyiv, Ukraine
[3]University of Urbino Carlo Bo, Urbino, Italy

METHODOLOGY FOR THE AUTOMATED DETECTION OF ANOMALOUS GEOSPATIAL ZONES IN SATELLITE IMAGERY USING STATISTICAL ANALYSIS AND A CUSTOM QGIS PLUGIN

(Представлено членом редакційної колегії д-ром геогр. наук, проф. Д.О. Ляшенком)

Background. *This article presents a methodology for the automated detection of anomalous geospatial zones, implemented as a plugin for the QGIS geographic information system. The developed tool enhances the efficiency of spatial analysis and enables the rapid identification of areas with potential changes for monitoring natural and anthropogenic processes.*

Methods. *The proposed approach is based on thresholding and statistical analysis of satellite imagery within the QGIS environment. The plugin provides interactive adjustment of image processing parameters and automatically detects geodynamic anomalies, which are then vectorized and delivered to the user for further analysis. The algorithm utilizes Python libraries (NumPy, SciPy, GDAL, PyQt, QGIS API) to handle various types of satellite data and applies standard deviation-based criteria to identify anomalous areas.*

Results. *The testing of the plugin developed by the authors confirmed its effectiveness in processing satellite imagery types such as InSAR, thermal infrared (TIR), and NDWI-based images. The plugin successfully identified areas of vertical displacement of the Earth's surface, detected thermal anomalies, and delineated regions with moisture deficits. This approach substantially improves the accuracy of geospatial analysis.*

Conclusions. *The developed plugin is an effective tool for the automated monitoring of changes in the Earth's surface and the assessment of hydrogeological conditions. Its integration within the QGIS environment enables the efficient adjustment of analysis parameters and the generation of results in vector data format. Plugin testing confirmed its practical value and revealed potential directions for further improvement, particularly regarding the separate processing of positive and negative displacement values to enhance the accuracy of anomaly interpretation.*

Keywords: *automated detection, geospatial zones, QGIS plugin, satellite imagery, geodynamic anomalies, spatial analysis.*

Background

In the modern, rapidly changing world, various types of emergencies increasingly arise, including natural disasters, military conflicts, and man-made accidents. In such situations, rapid response is critically important, as it involves assessing the situation and making optimal or efficient decisions to mitigate negative consequences. However, the process of territorial assessment is often time-consuming and complex due to the large volume of data that must be processed, as well as the lack of effective tools for timely data collection and analysis.

Contemporary methods for analyzing satellite imagery play a key role in monitoring environmental changes, assessing anthropogenic impacts, and detecting geodynamic processes. Nonetheless, traditional approaches such as visual interpretation and manual digitization have significant limitations when dealing with large-scale areas or vast datasets. Their effectiveness is often compromised by the subjectivity of interpretation, dependence on the operator's qualifications, and the difficulty of reproducing results, which complicates long-term analysis and automated change mapping. Therefore, new tools capable of automating these processes and enhancing the accuracy of outcomes are needed to overcome these challenges and ensure timely analysis (Tempa, & Aryal, 2022).

Under these circumstances, the availability of a comprehensive tool capable of conducting rapid and accurate analysis of satellite images to detect destruction and assess the overall condition of affected areas becomes essential (MASAI Project, n.d.). Such tools represent a vital component for improving emergency response efficiency. The automation of satellite image analysis through the use of Geographic Information Systems (GIS) helps to minimize the shortcomings of traditional methods by standardizing the detection of anomalous zones that emerge as a result of image processing (Janz et al., 2021). In particular, geostatistical algorithms facilitate more accurate anomaly recognition, reduce the impact of data noise, and enhance overall analysis efficiency. The integration of such solutions into the QGIS environment opens new opportunities for automated monitoring of surface changes, especially in the context of hydrogeological condition assessments and the analysis of anthropogenic impacts (Ivanik et al., 2022).

This study presents a custom-developed plugin for the QGIS software that enables the identification of anomalous zones derived from satellite image processing – namely,

ISSN 1728-2713 (Print), ISSN 2079-9063 (Online)

areas that deviate from background values and indicate changes or anomalies within the studied region. A key feature of the plugin developed by the authors is its applicability to various types of satellite data. Specifically, the study demonstrates the use of the plugin with InSAR images, thermal infrared (TIR) imagery, and optical indices derived from multispectral images (e.g., NDWI in the green and near-infrared (NIR) bands). The plugin is lightweight and user-friendly, requiring no additional pre-processing or complex computations. The user simply uploads an image, defines parameters for extracting polygons with anomalous values, and the plugin automatically performs the analysis and generates results. The plugin is freely available under an open-access license at https://github.com/rnrhs/autocountour_qgis_plugin (Marhes, 2025), ensuring its broad accessibility to researchers and professionals working in the fields of remote sensing and geospatial technologies. Its open-source nature also allows for easy modification, extension of functionality, and integration into diverse analytical workflows, which is a crucial aspect for supporting both scientific research and applied engineering practices.

The primary objective of the developed plugin is the automated detection of anomalous zones that exceed predefined threshold values, separating them from the main data array that does not meet the anomaly criteria. The threshold serves as a criterion for identifying deviations from the average or statistically expected values, enabling the extraction of geospatial objects with abnormal displacements or other parameters that warrant further analysis.

Methods

The algorithm governing user interaction with the plugin interface comprises a series of sequential steps designed to enable efficient processing of satellite imagery and the detection of zones with potential geodynamic anomalies (Fig. 1).

The image processing workflow within the developed plugin begins with its launch in the QGIS environment. Prior to this, the plugin must be installed following the official QGIS guidelines (QGIS Project, 2024). Subsequently, the user selects the raster image to be processed and adjusts the sensitivity parameters to configure anomaly detection settings. As the user modifies the sensitivity threshold, corresponding changes are dynamically visualized on the map, allowing threshold values to be fine-tuned through iterative selection to enhance the accuracy of anomaly detection. The final output is generated in the form of vector data, which is well-suited for further spatial analysis.

Fig. 1. Schematic representation of the sequence of user-side operations

The proposed QGIS plugin algorithm, grounded in statistical analysis and geoinformation approaches, facilitates the effective identification of anomalies in raster data by employing threshold-based and statistical techniques for the automated detection of anomalous regions in satellite imagery, followed by automatic vectorization of the results. The core principle of the algorithm is the assumption that anomalous values can be identified as deviations from the average statistical level, defined within a specified threshold coefficient.

Threshold analysis is based on determining a value beyond which the data are considered anomalous (Folini, Lenzi, & Biraghi, 2022). The threshold can be set manually or computed adaptively depending on the data distribution. Although this method is relatively straightforward to implement, it requires appropriate threshold selection to avoid false positives. The main stages of the threshold analysis include:

- noise removal and interpolation of missing values;
- determination of the threshold value – which can be specified by the user or automatically calculated (e.g., as a percentage of the maximum deviation or based on a histogram of data distribution);
- application of the threshold criterion – comparing each pixel to the threshold and highlighting zones exceeding this level, followed by contour smoothing;
- filtering of spurious regions.

Statistical analysis is employed to identify areas that significantly deviate from the average level of values. One common approach involves the use of standard deviation to detect anomalies:

$$x \mid x > \mu + k\,\sigma, \qquad (1)$$

where μ denotes the mean value, σ the standard deviation, and k a coefficient defining the anomaly level.

This method accounts for statistical properties of the data distribution, thereby improving detection accuracy (Folini, Lenzi, & Biraghi, 2022).

Numerous statistical methods for anomaly detection are based on conventional statistical thresholds, classifying anomalies into weak (approximately 5 %) and strong (approximately 0.3 %) categories. These classifications rely on standard deviation metrics and the assumption of normal distribution (Cleveland, 1993; Zhukov, 2008; Meng et al., 2017), and form the basis for data classification. These principles underpin the proposed plugin algorithm for detecting anomalous zones in satellite imagery.

The algorithm is implemented in the QGIS plugin using several Python libraries:

- NumPy – for efficient statistical computations and array processing;
- SciPy – for mathematical analysis and spatial filtering techniques;
- GDAL – for handling geospatial data and raster image processing.

In addition to these statistical analysis libraries, the developed plugin also utilizes a number of other Python packages to ensure full functionality and seamless integration with QGIS. Notably, components from the PyQt library are imported to construct the graphical user interface for parameter configuration (QSettings), translations (QTranslator), core functionality (QCoreApplication), icon management (QIcon), and dialog windows (QAction).

For spatial data handling, the plugin uses QGIS libraries such as QgsProject, QgsRasterLayer, and QgsVectorLayer for managing projects and layers, QgsRasterBandStats for computing statistics, and QgsMessageLog for message logging. Additionally, the GDAL, OGR, and OSR libraries support the manipulation of raster and vector data, while NumPy provides the

computational backend. The plugin also integrates resources from an external file (resources.py) and implements a dialog window to facilitate user interaction (Fig. 2).

All raster and vector data processed within the system adhere to a unified coordinate reference system, which is essential for accurate integration and geospatial analysis. To ensure consistency, the plugin retrieves the coordinate system and projection information of the selected raster layer. Initially, the active raster layer is identified via the map layer control element (mMapLayerComboBox). The data source path of the selected layer is then obtained, and the corresponding raster file is opened using the GDAL library. The *GetProjection() method* is employed to extract the layer's projection description in Well-Known Text (WKT) format, which enables precise identification of the spatial parameters and coordinate system of the data.

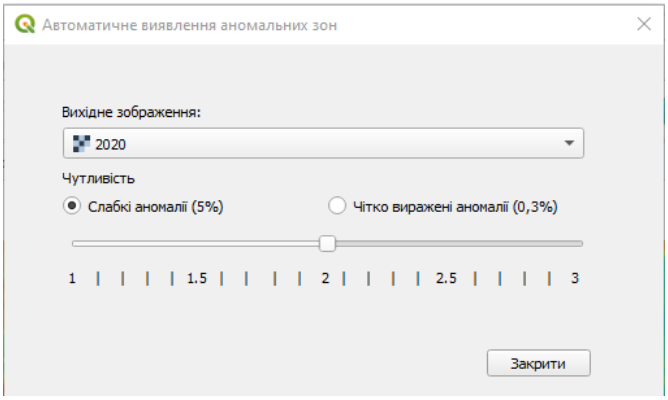

Fig. 2. User interaction dialog in the developed plugin

A detailed breakdown of the AutoContour plugin's functionality is provided to elucidate its underlying principles by separating it into distinct logical modules.

Plugin Initialization

The initialization process of the AutoContour plugin involves the import of essential libraries, including PyQt, the QGIS API, GDAL, OGR, and NumPy. At this stage, a reference to the QGIS interface is stored, enabling access to data and the ability to manage map layers. The plugin directory is also defined, and localization is configured based on the user's system settings. Variables are declared to store the paths of temporary raster and vector files that are generated and processed throughout the algorithm's execution. This design enhances the plugin's modularity and performance within the QGIS environment, while also preventing unnecessary file accumulation.

Graphical Interface and QGIS Integration

The integration of the plugin with the QGIS graphical interface is achieved through its registration in the software menu and the addition of the corresponding tools to the toolbar. This process is implemented using the *initGui() method*, which creates control elements such as buttons and menus, providing the user with access to the plugin's functionalities. The main element is the action (QAction), which is added to the toolbar and the 'Raster' menu, enabling the execution of the automatic contouring algorithm from the graphical interface. The plugin also supports the dynamic loading of localized resources, ensuring the correct display of interface elements according to the user's language settings.

For proper management of the plugin's operation, a mechanism for unloading is provided through the *unload() method*, which is responsible for clearing the interface and removing the corresponding menu items and buttons from the toolbar. User interaction with the algorithm is facilitated through the AutocountourDialog window, which allows the user to set processing parameters, such as the segmentation threshold. The window supports interactive adjustment of parameters, enabling real-time control over the analysis results. Thus, the developed architecture ensures flexible integration of the plugin into the QGIS environment and facilitates its use for spatial data analysis.

Raster Data Processing

The algorithm for processing raster data is based on their mathematical representation as a discrete two-dimensional function (Kotsiubivska, & Tymoshenko, 2019):

$$R: Z^2 \to R, \quad R(i,j) = r_{ij}, \tag{2}$$

where *R (i.j)* is the pixel value at position *(i.j)*, $r_{i.j}$ is the pixel intensity (e.g., reflectance, spectral brightness in a certain wavelength range, or another parameter).

The statistical analysis of the raster image begins with the calculation of its key characteristics, such as the average brightness value. The average brightness value for the entire raster image is calculated using the formula:

$$\mu = \frac{1}{N}\sum_{i=1}^{M}\sum_{j=1}^{N} r_{ij}, \tag{3}$$

where *M* and *N* correspond to the dimensions of the raster image (rows and columns, respectively), and the product $M \times N$ defines the total number of pixels in the image.

The average value defines the background of the image, enabling the identification of local deviations.

The standard deviation is determined using the formula:

$$\sigma = \sqrt{\frac{1}{N}\sum_{i=1}^{N}(I_i - \mu)^2}. \tag{4}$$

This parameter indicates the variability of brightness and is critical for the subsequent identification of anomalous zones.

Anomalous zones are identified using a statistical criterion based on deviations from the mean value to detect anomalous values in the case of a normal distribution of a random variable. This approach is widely used in the processing of satellite images and geospatial data analysis (Gavade, & Rajpurohit, 2021). According to this approach, values of the random variable that fall outside the range

$$\mu \pm k\sigma, \tag{5}$$

where μ is the expected value, σ is the standard deviation, and *k* is the anomaly coefficient, are considered potentially anomalous.

In this context, for raster data processing, this rule allows for the identification of areas where the intensity values significantly differ from the mean level, which may indicate the presence of natural or anthropogenic anomalies (Folini, Lenzi, & Biraghi, 2022). This method is based on the assumption of a Gaussian distribution of pixel intensity, which is typical for many natural phenomena and remote sensing of

the Earth (Hytla et al., 2009). Thus, the determination of anomalous zones is described by the formula:

$$I_i = \mu + k\sigma. \quad (6)$$

This allows for the identification of regions where the values substantially exceed the background level. The approach relies on the assumption of a normal distribution of pixel intensities, which is typical for natural processes and satellite data.

Raster image binarization involves obtaining a mask *M(i.j),* which is converted into a new raster file, where 1 corresponds to anomalous zones and 0 to the normal background:

$$M_{bin}(i,j) = \begin{cases} 255, & \text{if } M(i,j) = 1, \\ 0, & \text{if } M(i,j) = 0. \end{cases} \quad (7)$$

This mask allows for the visualization of anomalous areas and their storage in a standard format, such as GeoTIFF. At this stage, the projection and coordinate system of the input raster are assigned to the resulting mask.

Vectorization and Processing of Anomalous Zones

The process of vectorizing anomalous zones in a raster image is based on the *gdal.Polygonize() algorithm*, a function in the GDAL library that converts pixel regions with identical values into a set of closed polygons. Mathematically, this process can be represented as the construction of the set

$$\mathrm{P} = \{A_i\}_{i=1}^{N}, \quad (8)$$

where A_i denotes individual regions formed by connected pixels with the same intensity value, and *N* represents the total number of identified anomalous zones.

Vectorization allows the conversion of a discrete representation of spatial data into a more suitable form for further analysis, ensuring effective processing and storage of information in geospatial vector formats such as Shapefile or GeoJSON.

The vectorization algorithm consists of several key stages. The first stage employs a scan-line algorithm, which identifies the boundaries of anomalous objects through the sequential scanning of the raster image. Next, the connected components of each object are determined and grouped into closed contours based on the topological properties of pixel connections. The final stage involves saving the resulting contours in vector form, enabling further spatial analysis, such as the calculation of geometric characteristics, the determination of the area and perimeter of anomalous zones, and integration with other geospatial data. This approach ensures high analysis accuracy and enables the automation of the anomaly identification process in satellite images and other geospatial data.

Upon completion of the polygonization stage, the obtained vector objects undergo filtering to eliminate potential artifacts or noise that may have been generated during the analysis. The primary criterion for identifying such artifacts is the area of the polygon, which is determined using Gauss's formula (Gavade, & Rajpurohit, 2021):

$$S_i = \frac{1}{2}\left|\sum_{j=1}^{n}\left(x_j y_{j+1} - x_{j+1} y_j\right)\right|, \quad (9)$$

where S_i is the area of the polygon, x_j, y_j are the coordinates of its vertices, and *n* is the number of vertices of the polygon.

Among all identified anomalous zones, the polygon with the largest area is selected, as it is most likely to be an artifact or noise formation. If its area significantly exceeds the average area of other objects, it is removed from further analysis. The remaining polygons are preserved for further processing and interpretation, enhancing the accuracy and reliability of the geospatial analysis results.

The final step is to save the resulting vector objects as a new layer in Shapefile format.

Temporary File Management

During the operation of the plugin, temporary files are automatically created and managed, including the generation of directories for storing intermediate raster and vector data. This process may increase memory load and impact data processing performance. To ensure optimal use of system resources, all temporary files are automatically deleted either after their utilization is complete or upon the closure of QGIS. This approach helps prevent the accumulation of redundant data, enhances disk space efficiency, and minimizes memory usage, which is particularly critical when processing large volumes of geospatial data.

The aforementioned data processing sequence on the system side relies on active modules for raster and vector data that are executed each time user-defined parameters are modified (Fig. 3). These parameters include the selection of the raster layer and the specification of a sensitivity threshold (Jain, Duin, & Mao, 2000). The defined sensitivity threshold determines the subset of data that satisfies the following expression:

$$\left|\frac{raster_{array} - \mu}{\sigma}\right| > \theta, \quad (10)$$

where the expression considers only positive values, as the modulus (interpreted by the system as the *abs* function) denotes the absolute value function. Here, $raster_{array}$ refers to the data matrix, μ is the mean of the matrix, σ is the standard deviation, and θ is the sensitivity coefficient (threshold). The computed results are immediately made available to the user in the form of polygons representing anomalous values within the data array.

Thus, each change in user parameters triggers a processing cycle of raster and vector modules in sequence, enabling the visual evaluation of anomalous values based on the specified threshold.

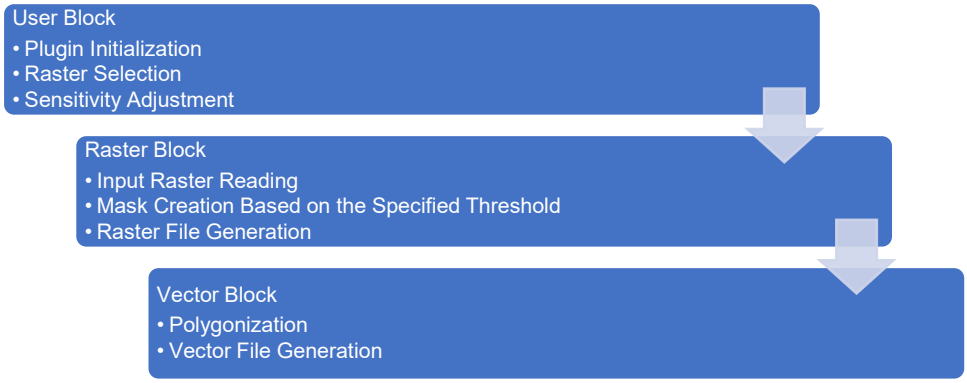

Fig. 3. Schematic representation of the sequence of processes executed on the system side

Results

The results produced by the developed plugin (Fig. 4) were analyzed based on three types of satellite imagery: InSAR images for detecting vertical surface displacements, thermal infrared (TIR) images for determining land surface temperature (LST), and multispectral images in the green and near-infrared (NIR) spectral bands used to calculate the Normalized Difference Water Index (NDWI). The automated analysis of these imagery types using the plugin significantly simplifies the interpretation of spatial data, thereby enhancing research efficiency and supporting timely decision-making in the fields of environmental monitoring and land management.

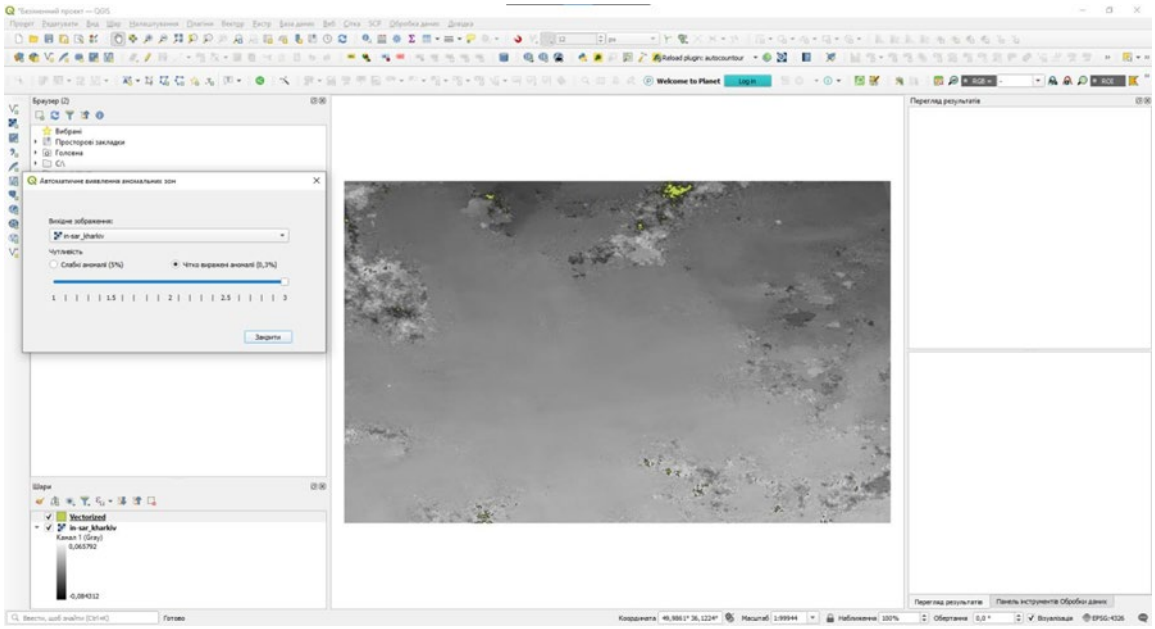

Fig. 4. General view of the developed plugin in QGIS software

Case 1: InSAR Imagery Analysis

The modern development of engineering infrastructure and urban areas is accompanied by substantial anthropogenic pressure on the Earth's surface. Construction of bridges, dams, underground utilities, and high-rise structures disturbs the natural equilibrium, potentially leading to vertical displacements of the Earth's crust, localized deformations, or even catastrophic failures (Kril, 2017). Accordingly, monitoring such processes is critically important for ensuring infrastructure safety and sustainable development.

The analysis of Sentinel-1 satellite imagery using the Differential Interferometric Synthetic Aperture Radar (D-InSAR) method serves as a powerful tool for detecting vertical surface displacements, particularly in urbanized environments (Minh, Hanssen, & Rocca, 2020). This method enables the detection of even minor topographic changes with high precision, making it indispensable for assessing geodynamic processes, risk forecasting, and informed decision-making in urban planning and engineering geology. The application of D-InSAR is especially relevant in zones of active construction, seismically hazardous areas, regions of underground resource extraction, and locations prone to subsidence or landslides (Kruglov, Hudak, & Kruhlov, 2025). The use of Sentinel-1 radar imagery facilitates the observation of displacement dynamics over time and the identification of long-term deformation trends.

In this case, the plugin was supplied with an InSAR satellite image of the city of Kharkiv (Fig. 5a), processed using the D-InSAR technique. After processing, the plugin automatically identified anomalous values indicating the presence of surface changes within the study area. These anomalies may correspond to vertical crustal deformations caused by either natural or anthropogenic factors. The resulting output provides a visualization of elevation changes, enabling detailed examination of geodynamic processes in the region and further analysis of zones exhibiting anomalous displacements (Fig. 5b). The statistical characteristics derived from the processed InSAR imagery demonstrate significant variability in surface displacement values (Table 1). The largest anomalous area (polygon ID 193) shows a minimum displacement of –0.11 m, a maximum of –0.05 m, and an average of –0.07 m. Such negative values may indicate ground subsidence. Other significant polygons, such as ID 205 and ID 400, exhibit similar average values, pointing to the existence of subsiding areas in the region. The range of values in most cases does not exceed 0.03 m, indicating the localized nature of the detected changes.

Displacements with positive values (e.g., polygons ID 799, 632, and 596) indicate uplift of the Earth's surface. For instance, polygon ID 632 demonstrates a minimum value of 0.05 m, a maximum of 0.08 m, and a mean value of 0.05 m. Such values may reflect specific geodynamic processes, including ground uplift or deformation driven by anthropogenic or natural factors. In all cases, the standard deviation remains relatively low (0.01–0.004 m), confirming the uniformity of changes within each identified polygon. Overall, the resulting characteristics allow for a quantitative assessment of the extent of surface changes and facilitate the identification of zones requiring continued monitoring.

Thus, the automation of D-InSAR data analysis within QGIS significantly enhances the efficiency of deformation monitoring while ensuring a more objective, reproducible, and scalable approach to assessing geodynamic processes across various territories. This enables timely detection of potentially hazardous zones, which is especially important for areas undergoing intensive urban development or those with complex engineering and geological conditions.

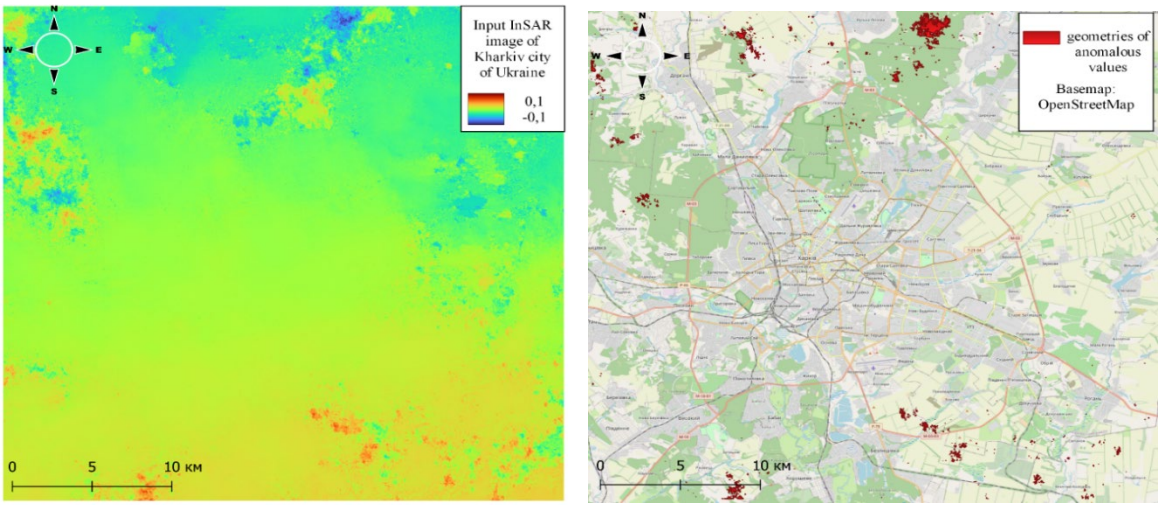

a b

Fig. 5. Input image processed using the D-InSAR method (a); detected anomalous zones of vertical displacement (b)

Table 1

Polygon ID	Area, m²	Min	Max	Mean	Standart deviation	Range	Sum of squares
193	1536244	-0,11	-0,05	-0,07	0,01	0,05	1,87
205	169109	-0,09	-0,05	-0,07	0,01	0,03	0,1
799	147380	0,05	0,07	0,05	0,01	0,03	0,08
400	131831	-0,08	-0,05	-0,07	0,01	0,03	0,09
632	93853	0,05	0,08	0,05	0,01	0,03	0,05
82	66415	-0,08	-0,05	-0,06	0,01	0,03	0,03
369	60226	-0,09	-0,05	-0,07	0,01	0,03	0,07
596	59012	0,05	0,08	0,06	0,01	0,03	0,05
308	49301	-0,08	-0,05	-0,06	0,004	0,02	0,02
840	42160	0,05	0,07	0,06	0,01	0,03	0,02
269	41401	-0,08	-0,05	-0,06	0,004	0,02	0,02
506	40645	-0,08	-0,05	-0,06	0,004	0,02	0,01

Case 2: Landsat 8/9 (Thermal Infrared Sensor)

Satellite imagery acquired via the Thermal Infrared Sensor (TIRS) onboard Landsat 8/9 satellites serves as a critical data source for monitoring temperature variations on the Earth's surface. This is particularly relevant in the context of climate change, as such data enable the identification of warming trends, overheating in urbanized areas, and fluctuations in soil moisture (Lischenko, Pazynych, & Filipovych, 2017; Filipovych, & Shevchuk, 2018).

Thermal sensor data, especially from TIRS, are employed for the monitoring of geothermal resources, detection of elevated temperatures in zones of volcanic activity, and analysis of terrain changes related to geological displacements and ground deformation. Furthermore, these data are valuable for assessing the ecological state of landscapes – particularly in areas affected by mining – where surface temperature shifts may indicate land degradation. Thermal imagery is also instrumental in detecting and forecasting exogenous processes such as erosion or landslides, as well as in evaluating anthropogenic impacts and pollution caused by human activities (Vivaldi et al., 2022). Additionally, thermal data contribute to climate change modeling and the analysis of urbanization effects, especially in detecting urban heat islands.

The analysis of Land Surface Temperature (LST) using the developed plugin includes the application of criteria for detecting minor anomalies, comprising no more than 5 % of the total dataset. The input image (Fig. 6a) is an atmospherically corrected Landsat product representing LST in degrees Celsius for the year 2020. The study area is located in the central part of Kyiv Oblast and is characterized by extensive agricultural land use, which has a notable environmental impact on surrounding ecosystems – particularly the Supiy River – and features a clearly defined urban heat island in the city of Yahotyn, Kyiv Oblast, Ukraine.

The input thermal image (Fig. 6a) has the following characteristics: maximum temperature of 32.79 °C, mean temperature of 23.08 °C, minimum temperature of 14.07 °C, temperature range of 18.72 °C, and a standard deviation of 3.37 °C. Based on these metrics, 182 anomalous polygons were identified, each containing values that meet the predefined anomaly criteria. In total, the number of pixels with anomalous values amounts to 21.62 out of 455.60 (4.75 %).

The analyzed image exhibits a distinct spatial heterogeneity in thermal conditions, reflecting the complex interaction of natural and anthropogenic factors. The maximum recorded temperature is 32.79°C, the minimum is 14.07 °C, and the mean value is 23.08 °C, with a temperature range of 18.72 °C and a standard deviation of 3.37 °C (Tab. 2). In total, 182 anomalous figures were identified, occupying 21.62 pixels out of 455.60, representing 4.75 % of the total image area. All anomalous areas were classified into two categories: low-temperature anomalies (ranging from 14.06 °C to 16.33 °C), primarily associated with reservoirs and water bodies, and high-temperature anomalies (ranging from 29.45 °C to 32.79 °C), typical for dry open surfaces such as farmland and urban areas.

This thermal segmentation is also evident in the detailed analysis of selected features: for example, ID 159 and 88 show average temperatures of 14.81 °C and 15.37 °C, respectively, characteristic of moist or aquatic surfaces, whereas areas such as ID 109, 160, and 139 display elevated mean values above 30 °C, corresponding to dry open territories or urban zones. The variation in

standard deviation within the range of 0.27–0.71 °C indicates differing levels of temperature uniformity across individual geospatial objects. Large spatial structures, such as ID 159, exhibit stable temperature gradients, which are crucial for the comprehensive analysis of landscape thermal conditions (Fig. 6b).

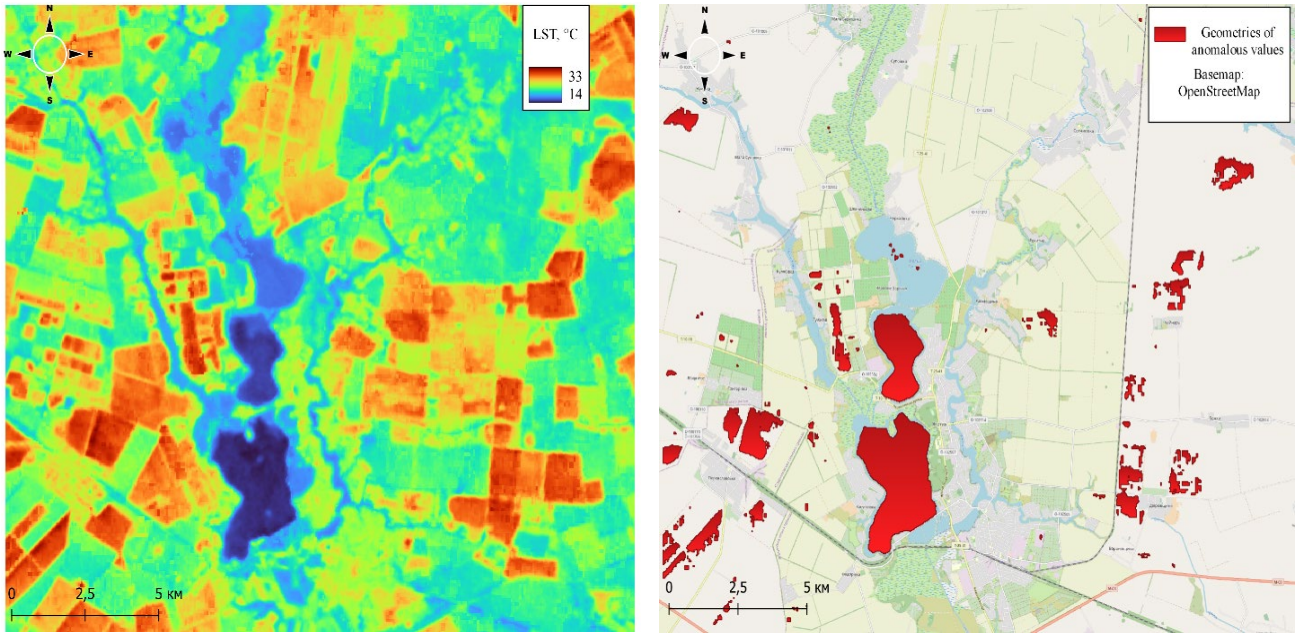

a b

Fig. 6. Input LST image (a); detected anomalous zones of high and low temperature (b)

Table 2

Polygon ID	Area, m²	Min	Max	Mean	Standart deviation	Range	Sum of squares
159	7453792	14,07	16,33	14,81	0,4	2,27	1344,38
88	3057343	14,49	16,33	15,37	0,38	1,85	492,43
109	1260731	29,83	32,79	30,76	0,65	2,96	581,46
26	683546	29,83	31,43	30,23	0,33	1,6	83,48
160	624957	29,83	32,47	30,68	0,71	2,64	345,52
17	454758	29,83	31,3	30,26	0,28	1,47	40,33
139	434077	29,83	31,96	30,5	0,44	2,13	93,28
102	433149	29,83	31,09	30,34	0,32	1,27	48
126	355727	29,83	31,21	30,25	0,35	1,38	48,54
79	329596	29,83	31,97	30,56	0,41	2,14	62,27
51	326010	29,83	31,49	30,24	0,38	1,66	50,99
113	285461	29,83	31,71	30,73	0,41	1,88	53,64

The application of the developed plugin significantly enhanced the efficiency of detecting geospatial objects with anomalous thermal characteristics based on user-defined criteria, thereby ensuring higher accuracy and timeliness in surface temperature monitoring. The obtained results can serve as a robust analytical foundation for forecasting climate trends, assessing ecological risks, and planning the rational use of land resources.

Case 3: Normalized Indices from Multispectral Imagery

As in the previously discussed cases, anomalous values help to identify the most affected zones characterized by specific index responses. In this instance, the Normalized Difference Water Index (NDWI) was used to detect surface water bodies (McFeeters, 1996); however, the use of other indices – such as NDVI, NDSI, NDDI, among others – can be beneficial for a wide range of thematic applications.

The area under investigation is located near the city of Yahotyn in Kyiv Oblast (Fig. 7a), along the Supiy River (Ukraine), which is known to experience periodic suffosion-induced subsidence (Marhes, 2024). The study of such physical processes in this region is of high relevance, as they are widespread on the left bank of the Dnipro River and exert a negative impact on agricultural productivity. NDWI was specifically selected due to its sensitivity to moisture accumulation in microdepressions formed by subsidence (Trofymenko et al., 2024).

NDWI values were derived from a PlanetScope satellite image (Planet Team, 2025), revealing predominantly dry or minimally moist areas with only limited evidence of water presence. Using the developed plugin, it was possible to visualize local terrain depressions – particularly bowl-shaped formations – where moisture accumulation was detected (Fig. 7b). In some instances, weakly expressed forms of linear erosion were also observed, further indicating irregularities in the surface hydrological regime. NDWI, which is responsive to the moisture content of vegetation and open water bodies, yielded uniformly negative values across the sample, ranging from –0.72 to –0.37. This confirms the predominance of dry soils or vegetation lacking free surface water.

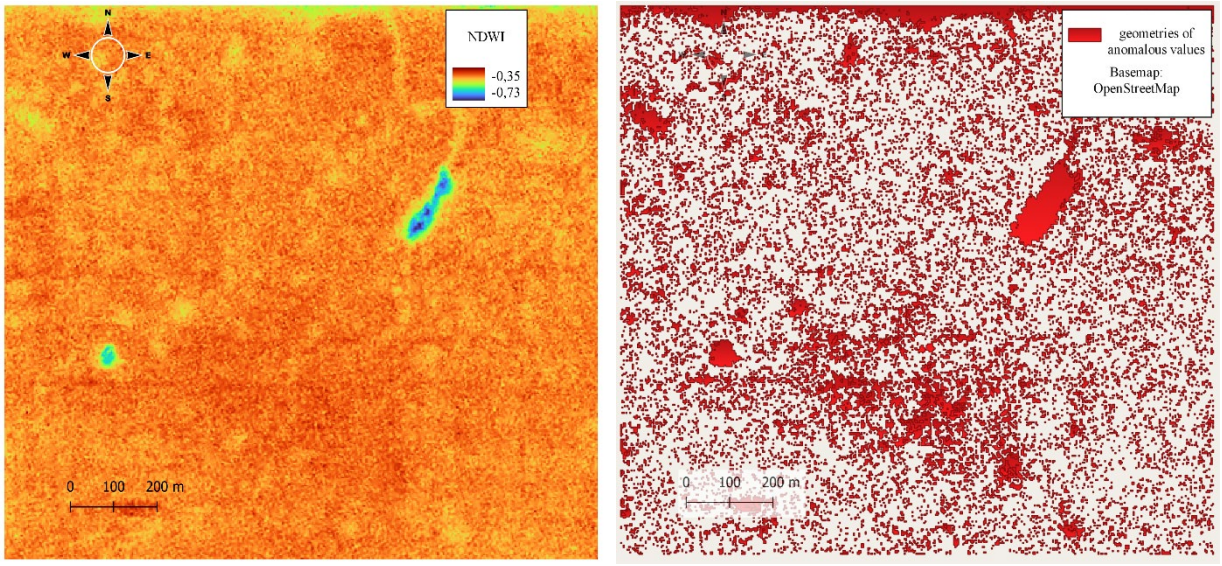

a b

Fig. 7. Input NDWI image (a); Detected anomalous (critical) zones in the image (b)

Analysis of the statistical data (Table 3) reveals a degree of heterogeneity across the studied areas. The largest zone is represented by object ID 580, covering 35,057 pixels, with an average NDWI value of –0.5 and a relatively narrow range (0.2), indicating a relatively homogeneous moisture condition. In contrast, object ID 4294 is characterized by the highest standard deviation (0.07) and a broader range (0.31), likely due to the presence of varying surface types or local hydrological contrasts. Other zones, particularly those with an area below 2,500 pixels (e.g., ID 6228), display stable NDWI values with minimal dispersion, which is typical for small, homogeneous micro-landscapes. The dominance of negative NDWI values across the dataset further confirms the prevalence of arid or low-moisture microenvironments.

Table 3

Polygon ID	Area, m²	Min	Max	Mean	Standart deviation	Range	Sum of squares
580	35057	-0,6	-0,41	-0,5	0,02	0,2	1,3
4294	15426	-0,72	-0,42	-0,54	0,07	0,31	7,47
7362	4007	-0,43	-0,38	-0,41	0,01	0,05	0,05
2375	3836	-0,54	-0,43	-0,49	0,01	0,11	0,08
2636	3710	-0,55	-0,42	-0,49	0,01	0,13	0,06
6457	3071	-0,64	-0,47	-0,53	0,05	0,17	0,8
7820	2756	-0,43	-0,39	-0,42	0,01	0,04	0,03
7170	2630	-0,43	-0,39	-0,42	0,01	0,04	0,02
8608	2467	-0,43	-0,39	-0,42	0,01	0,04	0,02
6217	2062	-0,43	-0,38	-0,42	0,01	0,05	0,02
8962	2044	-0,43	-0,37	-0,41	0,01	0,06	0,03
6228	2008	-0,48	-0,39	-0,42	0,01	0,09	0,02

The statistical analysis of NDWI values indicates an overall low moisture content throughout the entire study area. These data may be used to identify drought-prone zones, track seasonal fluctuations in moisture regimes, or compare with other indices such as NDVI or NDBI. The most analytically valuable areas are those exhibiting high variability, which may serve as indicators of local environmental changes or anthropogenic impacts.

Discussion and conclusions

The development of effective methods for analyzing satellite imagery represents a key challenge in monitoring both natural and anthropogenic environmental changes. The proposed approach to automated anomaly detection is grounded in the application of statistical methods, enabling high accuracy and processing speed.

Traditional approaches to image analysis typically rely on visual interpretation and manual digitization of anomalous zones. However, this method is time-consuming, particularly when dealing with large datasets containing numerous anomalies. Manual identification becomes increasingly difficult over extensive or densely built-up areas. Moreover, the results of such analysis often depend on the researcher's expertise and subjective interpretation, introducing potential error. The lack of a standardized algorithm further complicates reproducibility, which is critical for long-term environmental monitoring. Visual methods also fall short in handling large volumes of spatial data and accounting for spatial deformation patterns.

Given these limitations, the development of a plugin for QGIS that automates the identification of anomalous displacement zones is a timely and relevant solution. Automation allows for the standardization of analytical procedures, increased anomaly detection accuracy, and significant time savings. The integration of machine learning algorithms and geostatistical methods within the plugin enhances the precision of anomaly recognition and helps reduce data noise. Moreover, coupling the plugin with other geoinformation modules facilitates comprehensive analysis of interactions between surface deformations and influencing factors such as hydrogeological conditions or anthropogenic pressure.

The developed QGIS plugin streamlines satellite image analysis and greatly simplifies the identification of anomalous

zones. Its core functionality includes the use of threshold and statistical analysis methods to detect changes in geospatial data, contributing to more objective assessments and standardized outcomes. In addition, the plugin supports various types of satellite imagery – including InSAR, thermal infrared, and normalized index data – making it a versatile tool for a broad spectrum of researchers.

The algorithmic implementation is based on Python libraries such as NumPy, SciPy, and GDAL, which enable complex analytical computations to be seamlessly integrated into the QGIS environment. The use of thresholding and standard deviation calculations permits adaptive parameter tuning for anomaly detection, thereby reducing the likelihood of false positives.

Practical testing of the plugin has demonstrated its effectiveness in the context of automated surface change monitoring and hydrogeological assessment. Thanks to its intuitive graphical interface, users can easily configure analysis parameters and obtain results in the form of vector data, ready for further processing.

The testing process also generated ideas for future improvements. In particular, it was suggested to implement separate processing of positive and negative index or displacement values. This approach allows for consideration of the differing nature of physical processes or phenomena that produce anomalies of opposite signs – for example, ground subsidence versus surface uplift caused by anthropogenic or natural factors. Segregating these zones would enhance the accuracy of interpretation and improve decision-making based on the analytical results.

In summary, the developed plugin is an efficient tool for remote sensing research. It reduces the time required for satellite image analysis, increases accuracy, and standardizes approaches to environmental change assessment. Its integration into QGIS opens new avenues for geoinformation analysis, representing a promising direction for advancing monitoring methods for both natural and anthropogenic processes.

Authors' contribution: Vasyl Hudak – methodology, writing (review and editing), databases and data analysis, methodology; Serhii Marhes – conceptualization, data validation, graphic materials, writing (original draft); Vitalii Zatserkovnyi – formal analysis, revising of the manuscript, Mauro De Donatis – revision and editing.

Sources of funding. This research was conducted within the framework of the state-funded project "Integrated Models and Forecasting of Natural and Military Geohazards and Assessment of Their Impact on Critical Infrastructure" (State Registration No. 25BP049-01(M)).

References

Cleveland, W. S. (1993). *Visualizing data*. Hobart Press. https://www.hobartpress.com/visualizing-data

Filipovych, V., & Shevchuk, R. (2018). *Satellite technology for determining the heat load on the city in summer and ways to overcome it through green planning*. [Preprint]. https://doi.org/10.13140/RG.2.2.17113.08807

Folini, A., Lenzi, E., & Biraghi, C. A. (2022). Cluster analysis: A comprehensive and versatile QGIS plugin for pattern recognition in geospatial data. *International Archives of Photogrammetry, Remote Sensing and Spatial Information Sciences*, *XLVIII-4/W1-2022*, 151–157. https://doi.org/10.5194/isprs-archives-XLVIII-4-W1-2022-151-2022

Gavade, A. B., & Rajpurohit, V. S. (2021). Systematic analysis of satellite image-based land cover classification techniques: literature review and challenges. *International Journal of Computers and Applications*, 43(6), 514–523. https://doi.org/10.1080/1206212X.2019.1573946

Hytla, P. C., Hardie, R. C., Eismann, M. T., & Meola, J. (2009). Anomaly detection in hyperspectral imagery: Comparison of methods using diurnal and seasonal data. *Journal of Applied Remote Sensing*, 3(1), 033546.

Ivanik, O., Menshov, O., Bondar, K., Vyzhva, S., Khomenko, R., Hadiatska, K., Kravchenko, D., & Tustanovska, L. (2022). Integrated approach to modelling and assessing the landslide hazards at the regional and local scale in Kyiv urbanized area, Ukraine. *Modeling Earth Systems and Environment*. https://doi.org/10.1007/s40808-022-01447-x

Jain, A., Duin, R., & Mao, J. (2000). Statistical pattern recognition: A review. *IEEE Transactions on Pattern Analysis and Machine Intelligence*, 22(1), 4–37. https://doi.org/10.1109/34.824819

Janz, A., Jakimow, B., van der Linden, S., Thiel, F., & Dierkes, H. (2021). AVHYAS: A free and open-source QGIS plugin for advanced hyperspectral image analysis. In *2021 International Conference on Emerging Techniques in Computational Intelligence (ICETCI)*. IEEE. https://doi.org/10.1109/ICETCI51973.2021.9574057

Kotsiubivska, K., & Tymoshenko, V. (2019). Mathematical methods of image processing. *Digital Platform Information Technologies in Sociocultural Sphere*, *2*(1), 41–54. [in Ukrainian]. [Коцюбівська, К., & Тимошенко, В. (2019). Математичні методи обробки зображень. *Цифрова платформа. Інформаційні технології в соціокультурній сфері*, 2(1), 41–54]. https://doi.org/10.31866/2617-796x.2.1.2019.175653

Kril, T. (2017). Causes of some hazardous engineering geological processes on urban territories. In *E3S Web of Conferences* (Vol. 24). EDP Sciences. https://doi.org/10.1051/e3sconf/20172401009

Kruglov, O., Hudak, V., & Kruhlov, B. (2025, April). *Exploring D-InSAR Technology for Monitoring Soil Erosion: Case Study in Kharkiv Region*. Paper presented at the 18th International Conference Monitoring of Geological Processes and Ecological Condition of the Environment, European Association of Geoscientists & Engineers.

Lischenko, L., Pazynych, N., & Filipovych, V. (2017). Satellite monitoring of landslide development in the Pridnieprovska zone of Kyiv. *Ukrainian Journal of Remote Sensing*, 15, 111–120 [in Ukrainian]. [Ліщенко, Л., Пазинич, Н., & Філіпович, В. (2017). Супутниковий моніторинг розвитку зсувів у Придніпровській зоні м. Києва. *Український журнал дистанційного зондування*, 15, 111–120]. https://doi.org/10.36023/ujrs.2017.15.111

Marhes, S. (2024). Satellite geoecological analysis of the peat-swamp system of the Supii River. *Ideas and Innovations in Earth Sciences*, 24, 74–75. https://doi.org/10.30836/igs.iies.2024.34

Marhes, S. (2025). *Autocountour QGIS Plugin* (Version 1.0) [Computer software]. GitHub. https://github.com/rnrhs/autocountour_qgis_plugin

MASAI Project. (n.d.). *MASAI: Pioneering damage assessment through AI and satellite technology*. Retrieved July 8, 2025, from https://masai-project.eu/masai-pioneering-damage-assessment-through-ai-and-satellite-technology/

McFeeters, S. K. (1996). The use of the Normalized Difference Water Index (NDWI) in the delineation of open water features. *International Journal of Remote Sensing*, 17(7), 1425–1432. https://doi.org/10.1080/01431169608948714

Meng, C., Wang, Y., Zhang, X., Mandal, A., Zhong, W., & Ma, P. (2017). Effective statistical methods for big data analytics. In *Handbook of research on applied cybernetics and systems science* (pp. 280–299). IGI Global.

Minh, D. H. T., Hanssen, R., & Rocca, F. (2020). Radar interferometry: 20 years of development in time series techniques and future perspectives. *Remote Sensing*, 12(9), 1364. https://doi.org/10.3390/rs12091364

Planet Team. (2025). *PlanetScope NDWI image 20241024_090954_85_250a_3B_AnalyticMS_SR_8b_harmonized_clip*. Planet Labs PBC. https://www.planet.com/nextgenplanetscope/

QGIS Project. (2024). *Fetching plugins*. QGIS Documentation. https://docs.qgis.org/3.40/en/docs/training_manual/qgis_plugins/fetching_plugins.html

Tempa, K., & Aryal, K. R. (2022). Semi-automatic classification for rapid delineation of the geohazard-prone areas using Sentinel-2 satellite imagery. *SN Applied Sciences*, 4(1), 141. https://doi.org/10.1007/s42452-022-05028-6

Trofymenko, P., Tomchenko, O., Poralo, R., Zatserkovnyi, V., & Stakhiv, I. (2024). Remote identification of micro-depression relief forms and soil cover areas of agro-landscapes in the Polissya region of Ukraine with signs of hydromorphism. *Bulletin of Taras Shevchenko National University of Kyiv. Geology*, 1(104), 98–106. https://doi.org/10.17721/1728-2713.104.12

Vivaldi, V., Bordoni, M., Mineo, S., Crozi, M., Pappalardo, G., & Meisina, C. (2022). Airborne combined photogrammetry—infrared thermography applied to landslide remote monitoring. *Landslides*, 20(2), 547–560. https://doi.org/10.1007/s10346-022-01970-z

Zhukov, M. N. (2008). *Mathematical statistics and processing of geological data*. Vyshcha Shkola [in Ukrainian]. [Жуков, М. Н. (2008). *Математична статистика та обробка геологічних даних*. Вища школа].

Отримано редакцією журналу / Received: 26.02.25
Прорецензовано / Revised: 19.03.25
Схвалено до друку / Accepted: 30.06.25

Василь ГУДАК[1], асп.
ORCID ID: 0009-0002-7333-0409
e-mail: gudak_vasyl@knu.ua

Сергій МАРГЕС[2], асп.
ORCID ID: 0009-0004-2942-9406
e-mail: sergemarhes@gmail.com

Віталій ЗАЦЕРКОВНИЙ[1], д-р техн. наук, проф.
ORCID ID: 0009-0003-5187-6125
e-mail: vitalii.zatserkovnyi@knu.ua

Мауро ДЕ ДОНАТІС[3], канд. геол. наук, доц.
ORCID ID: 0000-0002-9721-1095
e-mail: mauro.dedonatis@uniurb.it

[1]Київський національний університет імені Тараса Шевченка, Київ, Україна
[2]Центр аерокосмічних досліджень Землі Інституту геологічних наук,
Національна академія наук України, Київ, Україна
[3]Університет Урбіно "Карла Бо", Урбіно, Італія

МЕТОДОЛОГІЯ АВТОМАТИЗОВАНОГО ВИЯВЛЕННЯ АНОМАЛЬНИХ ГЕОПРОСТОРОВИХ ЗОН НА СУПУТНИКОВИХ ЗНІМКАХ ІЗ ВИКОРИСТАННЯМ СТАТИСТИЧНОГО АНАЛІЗУ ТА СПЕЦІАЛІЗОВАНОГО ПЛАГІНА ДЛЯ QGIS

В с т у п . ***Представлено методологію автоматизованого виявлення аномальних геопросторових зон, реалізовану у вигляді плагіна для геоінформаційної системи QGIS. Розроблений інструмент підвищує ефективність просторового аналізу та забезпечує швидку ідентифікацію територій з потенційними змінами для моніторингу природних і техногенних процесів.***

М е т о д и . ***Запропонований підхід базується на використанні порогового та статистичного аналізу супутникових знімків у середовищі QGIS. Плагін забезпечує інтерактивне налаштування параметрів обробки зображень та автоматично виявляє геодинамічні аномалії, які після векторизації надаються користувачу для подальшого аналізу. Алгоритм використовує бібліотеки Python (NumPy, SciPy, GDAL, PyQt, QGIS API) для обробки різних типів супутникових даних і застосовує критерії на основі стандартного відхилення для виявлення аномальних ділянок.***

Р е з у л ь т а т и . ***Тестування розробленого авторами плагіна підтвердило його ефективність під час обробки супутникових знімків типів InSAR, теплових інфрачервоних (TIR) та знімків на основі індексу NDWI. Плагін успішно ідентифікував зони вертикальних зміщень земної поверхні, виявив температурні аномалії та окреслив області з дефіцитом вологи. Такий підхід суттєво покращує точність геоінформаційного аналізу.***

В и с н о в к и . ***Розроблений плагін є ефективним інструментом для автоматизованого моніторингу змін земної поверхні та оцінки гідрогеологічних умов. Його інтеграція в середовищі QGIS дає змогу оперативно налаштовувати параметри аналізу та отримувати результати у форматі векторних даних. Тестування плагіна підтвердило його практичну цінність і виявило потенційні напрями для подальшого вдосконалення, зокрема щодо роздільної обробки додатних і від'ємних значень зміщень для підвищення точності інтерпретації аномалій.***

К л ю ч о в і с л о в а : ***автоматизоване виявлення, геопросторові зони, плагін QGIS, супутникові зображення, геодинамічні аномалії, просторовий аналіз.***

Автори заявляють про відсутність конфлікту інтересів. Спонсори не брали участі в розробленні дослідження; у зборі, аналізі чи інтерпретації даних; у написанні рукопису; в рішенні про публікацію результатів.

The authors declare no conflicts of interest. The funders had no role in the design of the study; in the collection, analyses or interpretation of data; in the writing of the manuscript; or in the decision to publish the results.